CIRCUITS SYSTEMS SIGNAL PROCESSING
VOL. 21, NO. 3, 2002, PP. 225–242

DESIGN OF HIGH-PERFORMANCE WAVELETS FOR IMAGE CODING USING A PERCEPTUAL TIME DOMAIN CRITERION*

Marco A. M. Rodrigues[1], *Eduardo A. B. da Silva*[2] *and Paulo S. R. Diniz*[2]

Abstract. This paper presents a new biorthogonal linear-phase wavelet design for image compression. Instead of calculating the prototype filters as spectral factors of a half-band filter, the design is based on the direct optimization of the lowpass analysis filter using an objective function directly related to a perceptual criterion for image compression. This function is defined as the product of the theoretical coding gain and an index called the peak-to-peak ratio, which was shown to have high correlation with perceptual quality. A distinctive feature of the proposed technique is a procedure by which, given a "good" starting filter, "good" filters of longer lengths are generated. The results are excellent, showing a clear improvement in perceptual image quality. Also, we devised a criterion for constraining the coefficients of the filters in order to design wavelets with minimum ringing.
Key words: Image processing, wavelets, filter banks, perceptual quality.

1. Introduction

1.1. Image compression and quality evaluation

Image compression is very important in many areas of engineering activity involving telecommunications and storage. A very popular technique for image compression is the subband coding scheme, which maps the space domain image to the frequency domain, before the coding stage. Selection of a mapping method to yield the best performance is a critical issue that affects image quality as well as the coder design. Most of the best published results have been obtained by employing a wavelet transform, which is essentially an octave-band decomposition generated by the iteration of a two-band filter bank. The coefficients of the

[1] Centro de Pesquisas de Energia Elétrica - CEPEL, P.O. Box 68007, Rio de Janeiro, RJ, 21944-970, Brazil. E-mail: mamr@cepel.br

[2] EE/COPPE/Universidade Federal do Rio de Janeiro, P.O. Box 68504, Rio de Janeiro, RJ, 21945-970, Brazil. E-mail for da Silva: eduardo@lps.ufrj.br; E-mail for Diniz: diniz@lps.ufrj.br

* Received July 15, 2000.

Table 1. Comparison of the correlation coefficients between some wavelet features and both the *PSNR* and the subjective grade. The correlation coefficients presented are mean values, obtained for five different study cases

Feature	Correlation to *PSNR*	Correlation to subj. grade
Regularity of analysis/synthesis filter	0.22/0.20	0.46/0.35
Vanishing moments of analysis/synthesis filter	0.32/0.09	0.21/0.24
Aliasing energy of analysis/synthesis filter	0.19/0.24	0.44/0.35
Length of analysis/synthesis filter	0.20/0.06	0.19/0.16
Coding gain	**0.71**	0.26
PPR	0.30	0.68
Coding gain $\times$ PPR	0.58	**0.80**

two-band filter bank must be chosen according to some criterion. A work of major relevance is the maximally flat design technique [2], which produces wavelets with high values of regularity [8]. However, there are some criteria based on the time response of the wavelets, such as those in [17], where the shift invariance of the impulse response as well as the peak-to-sidelobe ratio is a factor of quality.

In [13], [14] a number of different criteria for wavelet evaluation were studied, as shown in Table 1. These criteria were compared to the peak signal-to-noise ratio (*PSNR*) [1] and to the subjective grades judged by seven expert viewers, using a process inspired by the ITU-R Recommendation 500. A set of 22 distinct wavelets was used for all five study cases. These study cases tested the influence of different images, coding techniques, and bit rates. The first column of Table 1 indicates that the coding gain is a good measure of the objective quality of the coded image, as its correlation to the *PSNR* is quite large. Similarly, the product of the coding gain and the peak-to-peak ratio (*PPR*, see Section 1.2 for a definition) shows a remarkable correlation figure to the subjective judgment. Note that regularity, which has been constantly used as a design objective, has a low correlation to objective measures as well as to subjective measures of image quality, (see Table 1).

The main result of this work is the use of these evaluation criteria to create a procedure for wavelet design. The results presented in [13], [14] are useful for wavelet design, because the values of both the coding gain (G_c) and the *PPR* are independent of the particular coding method employed. Therefore, the wavelet response can be optimized according to the function $G_c \times PPR$, which shows a high correlation to the subjective judgement of expert viewers. However, the manifold nature of the $G_c \times PPR$ surface makes this optimization extremely difficult to perform. In this work we present a techinique to overcome this problem.

Section 1 reviews the main concepts and equations needed to understand the work, Section 2 presents the algorithm and objective function used to calculate and optimize filters, and Section 3 presents the characteristics of the $G_c \times PPR$

function and uses them to propose a new algorithm to design filters of larger impulse response. Section 4 presents the main results.

1.2. Basic concepts

A two-subband perfect reconstruction filter bank is implemented with four filters: the analysis lowpass and highpass filters and the synthesis lowpass and highpass filters. Their z transforms are, repectively, $H_0(z)$, $H_1(z)$, $G_0(z)$ and $G_1(z)$, and the lengths of their impulse responses are L_0, L_1, L_1 and L_0, respectively.

Linear-phase filters are preferred for image compression, but two-subband perfect reconstruction orthogonal filter banks with linear-phase filters are trivial and have a very small coding gain. To circumvent this restriction, biorthogonal filter banks should be used instead.

For perfect reconstruction, such filter banks must satisfy the following conditions [16]:

$$H_0(z)\,H_1(-z) - H_0(-z)\,H_1(z) = 2z^{-2m+1} \tag{1}$$

$$\begin{bmatrix} G_0(z) \\ G_1(z) \end{bmatrix} = z^{2m-1} \begin{bmatrix} H_1(-z) \\ -H_0(-z) \end{bmatrix} \tag{2}$$

The pair $[H_0(z), H_1(z)]$ is said to be *complementary* if equation (1) holds. $H_0(z)$ is said to be *valid*, in the context of biorthogonality, if there exists a *complementary* $H_1(z)$. The conditions to achieve complementarity of the filters and the restrictions on filter length are detailed in [3], [15], [16].

When optimal bit allocation is used, it can be proved [5], [6] that the coding gain for subband coding systems with distinct subband resolutions is equivalent to

$$G_c = \frac{1}{\prod_{k=0}^{K-1} \left(\frac{A_k B_k}{\alpha_k}\right)^{\alpha_k}}, \tag{3}$$

where $\frac{1}{\alpha_k}$ is the decimation (and interpolation) rate in subband k. In this work the coding gain is computed assuming that the input signal is an autoregressive process of order 1 (AR(1)), and autocorrelation ρ. In this situation, it is found that [13]

$$A_k = \sum_{u=0}^{L_{h_k}-1} \sum_{v=0}^{L_{h_k}-1} h_k(u)\,h_k(v)\,\rho^{|u-v|} \tag{4}$$

$$B_k = \alpha_k \sum_{u=0}^{L_{g_k}-1} g_k^2(u),$$

where $h_k(n)$ and $g_k(n)$ are the analysis and the synthesis equivalent filters for subband k with lengths L_{h_k} and L_{g_k}, respectively.

It can be proved that, in orthogonal systems, optimal bit allocation is achieved if the average distortions (caused by quantization) per coefficient in all subbands are equal (an exponential quantizer model is assumed) [4]. This implies that a quantizer/coder that introduces the same distortion to all subbands (like the one in [12], which we used here) performs an optimal bit allocation in an orthogonal system. On the other hand, it can be shown that, in a biorthogonal system, a white quantization error with average energy e_k in band k appears on the reconstructed image as $e_k\sqrt{B_k}$, see equation (4). Therefore, in order for a coder like the one in [12] to perform an optimal bit allocation in a biorthogonal system, each one of the bands must be multiplied by $\sqrt{B_k}$ before quantization and divided by $\sqrt{B_k}$ after quantization. Failure to do so will decrease the signal-to-noise ratio (SNR) because the effect of the optimum bit allocation is lost. Note that, in most of the literature, this fact is neglected. This is not a problem if all $\sqrt{B_k}$ are close to one (as is the case of filter 9/7 from [2]). However, in a comparison of filters, failure to use this normalization of bands will handicap those filters whose $\sqrt{B_k}$ are not close to one, resulting in an unfair comparison.

The PPR is a measure of the damping in the wavelet oscillations towards its tails. Such oscillations directly influence the visualization of quantization errors after image reconstruction, especially *ringing*. Increasing the damping (and consequently the PPR) will decrease the visibility of errors [14]. In [17] a similar observation was made, and wavelets were chosen to have a small peak-to-sidelobe ratio.

The PPR is calculated from the synthesis wavelet because it is involved in signal reconstruction. In practice, it is computed from the equivalent filter corresponding to the iteration of $(i-1)$ lowpass interpolated filters and one highpass interpolated filter, using a number of stages i large enough for convergence. In fact, as shown in equations (1) and (2), all the filters in the filter bank are considered in the value of PPR. The PPR is defined as [13], [14]

$$PPR = \frac{2\,(x+y)}{((x+y)+(y+z))} \tag{5}$$

for symmetric wavelets (i.e., wavelets with even symmetry) and

$$PPR = \frac{2x}{x+y} \tag{6}$$

for antisymmetric ones (i.e., wavelets with odd symmetry). The values of x, y, and z are as they appear in Figure 1. For normal (i.e., damped) wavelets, the PPR can assume values in the interval $(1, 2]$. Note that the PPR is not defined for asymmetric wavelets (i.e., when the starting filters do not have the linear-phase property).

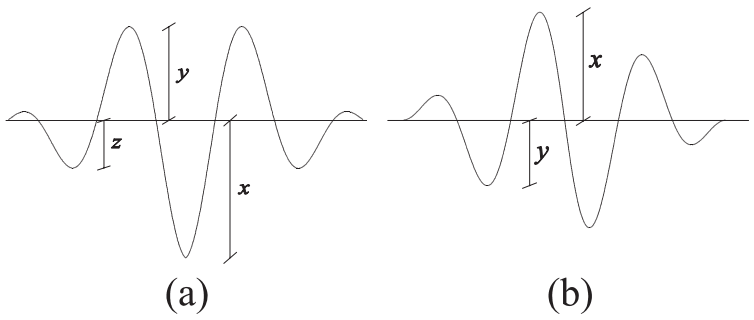

Figure 1. Parameters used in PPR calculation for wavelets with (a) even symmetry and (b) odd symmetry.

2. Wavelet design

2.1. Design of biorthogonal FIR linear-phase filters

The problem of biorthogonal two-band perfect reconstruction filter bank design is usually dealt with in the frequency domain using spectral factorization or lattice structures [7], [16]. For this work, however, the use of spectral factorization has some disadvantages: it is difficult to manipulate G_c and PPR on the polynomial $P(z) = H_0(z) H_1(-z)$; the number of spectral factors grows exponentially with the degree of $P(z)$; the factorization of $P(z)$ is numerically difficult when the number of zeros at $z = -1$ grows; and the resulting $H_0(z)$ and $H_1(z)$ are not necessarily optimal, even if $P(z)$ is optimized. Lattice structures like those presented in [7], [16], were not used here because it is difficult to manipulate their coefficients so that the entire optimization space is spanned.

In [3] a technique is presented for optimizing the coefficients of the filters directly if one of the two-band filter coefficients is kept constant. However, this process is suboptimal because just one of the filters is optimized.

For this work, we used an alternative technique to design the filters in which the impulse response of both the lowpass and the highpass filters can be directly optimized. Given a starting filter polynomial $H_0(z)$ that accepts a complementary polynomial, it is possible to calculate a unique $H_1(z)$ whose impulse response length is $L_1 \mid (L_1 \leq L_0)$ [3], [9], [16]; the detailed procedure is explained in the Appendix. Despite the restriction $(L_1 \leq L_0)$, this technique can be applied to design filter pairs with other length configurations, as shown in [9].

2.2. General optimization procedure

Throughout this work, all results are based on filter optimization. Except when otherwise noted, a quasi-Newton optimization method that uses the

BFGS (Broyden-Fletcher-Goldfarb-Shanno) formula [18] for updating the approximation of the Hessian matrix is employed. A program from the MATLAB Optimization Toolbox was used.

The general optimization procedure is performed as follows.

1. Choose the number of stages i in the wavelet transform.
2. Choose the lengths L_0 and L_1 according to the length constraints explained in [16].
3. Choose the initial lowpass filter impulse response $h_0(n)$. This filter must be *valid* and it must be chosen to provide a good starting point (Section 3 deals with this problem).
4. Extract the filter kernel, i.e., the free coefficients of the filter. These are coefficients $h_0(1)$ up to the central one. For example, if $L_0 = 6$, the kernel is composed of coefficients $[h_0(1), h_0(2)]$ (coefficient $h_0(0)$ is defined by filter normalization, $h_0(3) = h_0(2)$, $h_0(4) = h_0(1)$, and $h_0(5) = h_0(0)$).
5. Optimize filter kernel
   (a) Reconstruct the filter bank from the kernel, using equations (1) and (2). Equation (1) can be solved using the Appendix.
   (b) Calculate the objective function
   $$F = G_c(\rho, h_0(n), h_1(n), i) \times PPR(\widetilde{\psi}^{(i)}(t, g_0(n), g_1(n))), \qquad (7)$$
   where the term $\widetilde{\psi}^{(i)}(t, g_0(n), g_1(n))$ is an approximation of the synthesis wavelet using i iteration stages, and G_c and PPR are found as explained in Section 1.2.
   (c) Let the optimization algorithm suggest the new kernel or finish the optimization, if the end criteria is met.
   (d) If not finished, return to Step 5a.
6. Reconstruct the filter bank from the kernel, as in Step 5a.

In Step 5b, if an *invalid* filter $h_0(n)$ is found, this solution is avoided by assigning a low value to F.

2.3. Maximum PPR conditions

If we could define sufficient conditions so that a maximum PPR could be enforced to the filter coefficients, the objective function could be simplified to consider only the coding gain, i.e., $F = G_c(\rho, h_0(n), h_1(n), i)$.

First observe that in order to have a maximum PPR ($PPR = 2$), the wavelet must be anti-symmetric and y in Figure 1b must be zero, i.e., the wavelet must not oscillate beyond its first lobe. It means that the wavelet cannot change polarity between its beginning and its half point (or its point of symmetry). Also, observe that iterated (synthesis) wavelets are found by convolving interpolated versions

of $g_0(n)$ and $g_1(n)$ many times [16]. Then, a *sufficient* condition would be that both $g_0(n)$ and $g_1(n)$ have all coefficients with the same polarity, i.e.,

$$\operatorname{sign}(g_m(n)) = \operatorname{sign}(g_m(n+1)) \quad \forall\, n \in \left[0, L_{1-m} - 1\right],\ m \in [0, 1], \tag{8}$$

where L_m is the length of the analysis filter $h_m(n)$. However, in this situation, $G_1(n)$ will not have a zero at $z = 1$. Also, observing equation (2), we conclude that, in this case, $H_0(z)$ and $H_1(z)$ should be chosen such that their even indexed coefficients (those multiplied by even indexed powers of z) have inverse polarity to the odd indexed coefficients. One consequence of following this condition is that $H_0(z)$ would have no zeros at $z = -1$, i.e., it would not be a good lowpass filter. Fortunately, the condition in equation (8) is not *necessary*, and there are many examples of filters with $PPR = 2$ that do not follow it (e.g., filter $\mathbf{h} = [1, -6.489, -6.489, 1]$ has $PPR = 2$).

In practice, the most useful wavelets have a high coding gain, which generally implies good regularity and smooth appearance. Taking this into consideration, the calculation of the PPR can be simplified. After designing a large number of filters, we arrived at a less restrictive condition than that of equation (8). For maximum PPR, we conjecture that, if the coding gain is sufficiently high, the following conditions should be true:

- The lowpass synthesis filter impulse response is monotonically crescent, up to the central coefficient

$$g_0(n+1) - g_0(n) > 0 \mid n \in \left[0, \frac{L_1 - 1}{2}\right] \tag{9}$$

- The highpass synthesis filter has an impulse response with the same polarity up to the central coefficient

$$\operatorname{sign}(g_1(0)) = \operatorname{sign}(g_1(n)) \mid n \in \left[0, \frac{L_0 - 1}{2}\right]. \tag{10}$$

At first glance, these conditions are *sufficient*, not *necessary*. Sufficiency was tested in more than 10 000 filters for each filter size from $L = 5$ up to $L = 20$. The filter coefficients were chosen randomly, although following the preceding criteria. The test consisted in verifying whether these criteria are met by filter banks whose PPR is not maximum and where $G_c > 5$. No filter was found that did not meet the criteria. However, if there are no situations where PPR is maximum and these criteria are not met, the conditions would also be *necessary*. We applied a similar test to determine it and found not a single case (we also constrained G_c to be larger than five). So, we conjecture that, when the coding gain is sufficiently high, the preceding conditions should also be *necessary* for maximum PPR.

3. New design techniques based on similarities among surfaces of $G_c \times PPR$ for different dimensions

3.1. Surface mapping

Due to the manifold nature of the $G_c \times PPR$ surface, the optimization results are very dependent on the initial filter chosen. To seek a more general rule to define the initial filter we investigated the function defined by the product $G_c \times PPR$. The mapping process is achieved by repetitive calculation of the objective function from equation (7) for distinct values of the filter coefficients, over a region that includes the optimum filter for each dimension. The mappings were limited to two dimensions, to make it simple to understand the results. Seven distinct configurations of filter pairs were mapped (the L_0/L_1 convention is used for the impulse response length, and the number of zeros enforced or naturally ocurring at $z = -1$ is given in brackets): 5/3 [2], 7/5 [4], 4/4 [1], 6/6 [3], 5/3 [0], 6/6 [1], and 7/5 [2]. In all these cases, observation of the surface defined by the product $G_c \times PPR$ plotted against the filter h_0 coefficients has suggested that the coefficient space can be divided into regions, summarized as follows:

- The region of the global maximum, which is characterized when zeros other than those at $z = -1$ occur on the real axis. If there are only two zeros not at $z = -1$, they must be on the positive side. Otherwise, one-half of the real zeros must be positive and the other half negative.
- Regions of *degenerated* (see below) filters, which are characterized when zeros other than those at $z = -1$ occur on the unit circle.
- Regions of local maxima, which are characterized when zeros other than those at $z = -1$ occur in the complex plane (i.e., not on the real axis or the unit circle).

In the development of this work we optimized filter coefficients so that the performance of the resulting wavelets, expressed as the product $G_c \times PPR$, is maximized. In this process, we came across filters with long impulse responses which lead to wavelets with good performances. However, some of them do not have better performance than other already known wavelets, whose prototype filters are shorter. In such cases, the longer filters are said to be *degenerated*. *Degenerated* filters have, in general but not necessarily, a large spread in the values of their coefficients (for an example, see the following discussion relating to Figure 2) and the corresponding shorter filters can usually be obtained. (Note that through this work the filters are scaled so that the first coefficient is one. This enables easy understanding of the filter properties. However, when actually building the wavelets, the filter coefficients must be appropriately scaled.)

$$\begin{aligned} \mathbf{h}_{degenerated} &= [1, h_1(1), h_1(2), \ldots, h_1(2), h_1(1), 1] \\ \mathbf{h}_{reduced} &= [h_1(1), h_1(2), \ldots, h_1(2), h_1(1)] / h_1(1) \end{aligned} \tag{11}$$

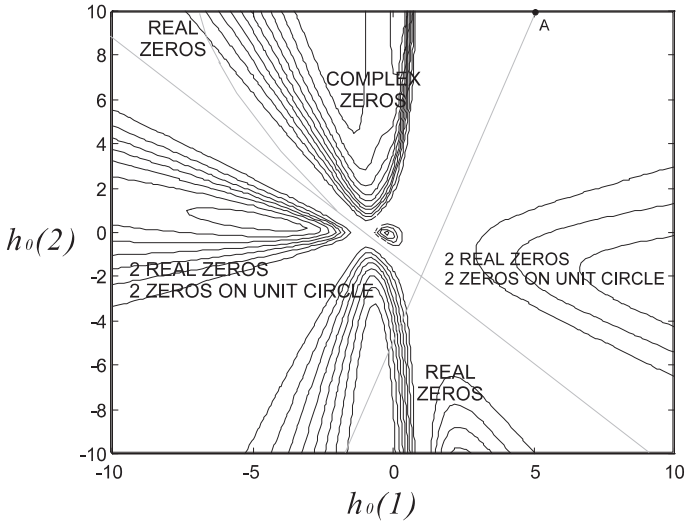

Figure 2. Contour map of $G_c \times PPR$ for the case $L_0 = 6, L_1 = 6$. The abscissa corresponds to parameter $h_0\,(1)$ and the ordinate corresponds to parameter $h_0\,(2)$. The regions inside the contour lines correspond to the maxima of the coding gain.

As an example, Figure 2 shows the mapping of $G_c \times PPR$ on the coefficient plane (actually the filter kernel $[h_0\,(1)\,, h_0\,(2)]$ as defined in Section 2.2 is used) for the length $L_0/L_1 = 6/6$. The concentric lines indicate distinct levels, with increasing values for curves near the center. Examining Figure 2, there are five distinct regions concerning zero positions. In the upper left corner, a region of real positive zeros is found; at the upper central part, there is a region of complex zeros (not on the unit circle); on the left and on the right sides, there are filters with two real zeros and two zeros on the unit circle; below there is a region of real zeros, two positive and two negative. Above point A there is a sixth region that does not appear in Figure 2, corresponding to real negative zeros. In the region of complex zeros there are *degenerated* filters. For example, $\mathbf{h} = [1, -2, 8, 8, -2, 1]$ has an acceptable performance, but it is a *degenerated* version of filter $[1, -4, -4, 1]$. When searching the surface of $G_c \times PPR$ in this region, the optimization algorithm described in Section 2.2 finds suboptimal filters. As an example, starting the optimization from the previous example, the filter $\mathbf{h} = [1, -176215, 1143369, 1143369, -176215, 1]$ is found. It is a *degenerated* version of $\mathbf{h} = [1, -6.49, -6.49, 1]$, which is the optimum filter of length 4. In the region of real zeros at the lower part of Figure 2, the best results are found. For example, filter $\mathbf{h} = [1, 2.250, -33.476, -33.476, 2.250, 1]$ is the optimum 6/6 filter. In the regions of real zeros in the upper left part and in the upper right part (not shown) of Figure 2, poor filters are found. In these filters all the zeros other

than those at $z = -1$ have the same polarity. The region where both real zeros and zeros on the unit circle occur generally corresponds to poor filters. Starting a search procedure in this region of the surface of $G_c \times PPR$, from any point, results in a failure to find a useful filter.

Filters in the region of global maximum have special properties. The first property is that these filters can be used in Step 3 of the optimization procedure of Section 2.2. The other property is related to filter growth and is detailed in Section 3.2. Although an analytical proof of these properties is not provided, their validity is demonstrated when comparing the results of the filter optimization using a gradient search to the results of the filter optimization using a *simulated annealing* algorithm, as explained in Section 4.

3.2. Design based on filter growth

By studying filters with long impulse responses reported in the literature, it was observed that some of them were *degenerated* (see Section 3.1) versions of other filters with shorter impulse responses. When reducing the filter length as in equation (11), it was observed that, when $h_{degenerated}$ has a good $G_c \times PPR$ performance, the reduced versions usually fall in the region of global maximum, according to what was observed when mapping the $G_c \times PPR$ surface. This means that there is a relationship between good filters of different lengths. Consequently, by reversing the process of filter reduction, it is conjectured that one can improve the performance of filters with short impulse responses by increasing their length. The process is as follows:

$$\begin{aligned} \mathbf{h}_{original} &= [1, h_1(1), h_1(2), \ldots, h_1(2), h_1(1), 1] \\ \mathbf{h}_{increased} &= [1, k, kh_1(1), kh_1(2), \ldots, kh_1(2), kh_1(1), k, 1]. \end{aligned} \tag{12}$$

The value of k can be determined by a single-variable optimization. From a geometric point of view, such a process consists of choosing a position (determined by the value of k) on a straight line that belongs to a space of higher dimension. The other variables, which are fixed, determine the placement of the line. In fact, it is expected that a good filter whose impulse response length is $L-2$ will have its coefficients close to the central terms of a good filter of length L, i.e., it is likely that these coefficients will place the above-mentioned line in a region next to a global maximum. The optimization of k helps in avoiding degenerated solutions. After determining the best k for $h_{increased}$, the filter response can be enhanced by performing the optimization of all its coefficients. Using this procedure recursively, as depicted in Figure 3, near-optimum filter responses of any length can be obtained. The algorithm can be described as follows.

1. Choose the starting filter coefficients (the filter has length L).
2. Choose the final filter length ($L + l$).
3. Initialize the starting filter as the current filter.

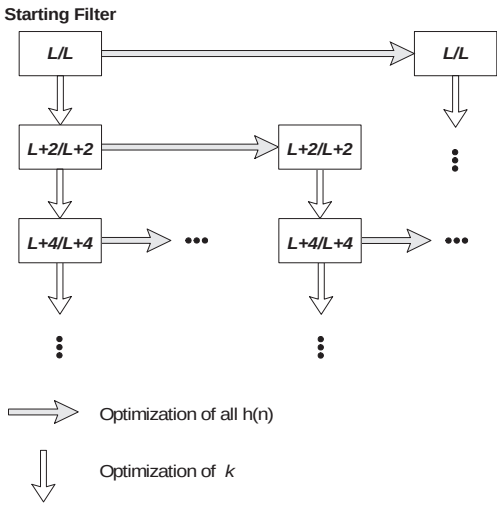

Figure 3. Basic operations used in design by growing the number of coefficients of the filter polynomial.

4. Create two new filters:
   (a) A filter resulting from optimization of the current filter coefficients
   (b) A filter resulting from increasing the current filter length and optimizing k.
5. Repeat Step 4 for each one of the two filters previously found. This step means that a tree of solutions with many branches will be created. The process stops when the length $(L + l)$ is achieved.
6. Choose the best solution encountered.

In Step 4, optimization is done as outlined in Section 2.2, and in step 4b, k is optimized instead of the filter kernel. If *invalid* filters, in the sense of Section 1.2, appear in Step 4, the problem can be dealt with by the optimization procedure of Section 2.2.

Note that this technique is more suitable for a filter whose impulse response has an even length. This is so because, in such a case, at least one zero at $z = -1$ is preserved when reducing the length of the impulse response as in equation (12). For filters whose impulse response has an odd length this is never the case, as shown below (consider $H_{original}(z)$ to have at least a zero at $z = -1$ and consider L to be odd), and a degree of freedom in the optimization is lost in order to enforce a zero at $z = -1$.

$$H_{original}(-1) = \sum (-1)^l h_{original}(l) = 0$$

$$H_{reduced}(-1) = \left(\sum (-1)^l h_{original}(l)\right) - \left(1 + (-1)^{L-1}\right) \neq 0.$$

Table 2. Characteristics of selected wavelets. Three stages used

Filters	L_0/L_1	G_c (dB)	PPR	$G_c \times PPR$	$PSNR$
Filter A from [14]	5/3	9.35	1.60	13.780	30.50
Filter from [2]	9/7	9.46	1.48	13.036	31.01
Filter F from [14]	10/14	9.61	1.59	14.478	31.17
Optimum $G_c \times PPR$	6/6	9.34	1.94	16.666	30.96
Optimized filter	8/8	9.36	1.93	16.704	30.83
Optimized starting from filter F	14/14	9.41	1.94	16.970	30.88

Furthermore, from the definition of PPR, we observe that antisymmetric wavelets (generated from the iteration of filters with even length impulse response) can have a PPR value equal to the maximum, 2. However, in the symmetric case (wavelets generated from the iteration of filters with odd length impulse response), such a value can never be reached. It happens because if y in Figure 1(a) is made very small in order to increase the PPR, the wavelet oscillations will be reduced, decreasing the coding gain. Note that in Figure 1(b), y can be made zero, and the wavelet still oscillates. This implies that the $G_c \times PPR$ performance obtained with symmetric wavelets tends to be inferior for antisymmetric wavelets. However, in the image processing literature, there are some filters whose impulse response has odd length, but which are said to result in good wavelets. A very popular example is the 9/7 filter cited in [2]. It has been reported to have better subjective and objective performance than most known wavelets. Its $G_c \times PPR$ figure is not among the highest ones (see Table 2), thus it is in apparent contradiction with our results. However, the advantage of the 9/7 filter when compared to other good filters is generally observed when the biorthogonal normalization (biorthogonal normalization is needed to achieve optimum bit allocation, see Section 1) is not carried out. This is so because the normalization factors B_k for the 9/7 filter bank are close to one, which is not the case for most filter banks with antisymmetric wavelets. Therefore, if biorthogonal normalization is carried out, the performance of filter banks with antisymmetrical wavelets is improved, as seen in Table 2.

4. Results

4.1. Maximum PPR

Using the conditions in equations (9) and (10) from Section 2.3, optimization was implemented using the coding gain as the objective function. To implement the test, the quasi-Newton method was replaced by a *simulated annealing* optimization algorithm, to ensure that the best results were obtained. This method is very robust in avoiding local solutions and it is independent of the starting point, but

Table 3. Performance of the best wavelets generated from the prototype filters found in our experiments. "Quasi-Newton" means that the starting filter coefficients were only optimized, no filter growth was necessary. A three-stage wavelet decomposition was used

Optimization	L_0/L_1	G_c	PPR	$G_c \times PPR$
Quasi-Newton	5/3	9.21	1.68	14.007
Quasi-Newton + filter growth	7/5	9.21	1.68	14.008
Quasi-Newton + filter growth	9/7	9.21	1.68	14.010
Simulated annealing	9/7	9.21	1.68	14.014
Quasi-Newton + filter growth	11/9	9.21	1.68	14.013
Simulated annealing	11/9	9.21	1.68	14.016
Quasi-Newton	13/11	9.26	1.67	14.045
Simulated annealing	13/11	9.19	1.69	14.026
Quasi-Newton	15/13	9.20	1.67	13.904
Quasi-Newton + filter growth	17/15	9.29	1.66	14.076
Quasi-Newton	4/4	8.99	2.00	15.832
Quasi-Newton	6/6	9.34	1.94	16.666
Quasi-Newton	8/8	9.36	1.93	16.704
Simulated annealing	10/10	9.29	1.98	16.818
Quasi-Newton + filter growth	10/10	9.34	1.95	16.722
Simulated annealing	12/12	9.33	1.96	16.857
Quasi-Newton + filter growth	12/12	9.34	1.96	16.854
Quasi-Newton	14/14	9.41	1.94	16.970
Simulated annealing	14/14	9.42	1.95	17.023
Quasi-Newton	16/16	9.43	1.93	16.925
Quasi-Newton + filter growth	18/18	9.40	1.95	16.998
Quasi-Newton + filter growth	20/20	9.44	1.93	16.952

its computational complexity is extremely high (note that, to avoid using brute force methods such as *simulated annealing*, a design algorithm is developed in Section 3.2). Unfortunately, the resulting filters are *degenerated*: the 6/6 filter has $G_c \times PPR = 15.832$, and its kernel is [116000, 757000]. Even for higher dimensions, filters perform no better than the 4/4 optimal filter (the 12/12 filter has $G_c \times PPR = 15.833$, and its kernel is [98.63, 828.2, 828.9, 73472, 481600]). Note also that the conditions for maximum PPR limit the search space a great deal as, for each new dimension, the space is halved. Furthermore, after designing a number of wavelets it was observed that the best filters do not have $PPR = 2$. Instead, they have PPR close to 2 (see Table 3). Although the test has shown that using a maximum PPR condition is not useful, its importance was to enable a better understanding of the features of the $G_c \times PPR$ function.

4.2. Filter growth

The best filters achieved with the design technique presented in Section 3.2 are shown in Table 3. To calculate the filters of Table 3, different starting filters

were used, such as the Haar filter pair, and some of the filters reported in [2], [14], [17], a total of 12. More than 100 filters were found when creating the branches referred to in the description of the algorithm. One can see that, although the value of $G_c \times PPR$ has a tendency to increase with filter length, there seems to exist an asymptotic behavior limiting this value to less than 18, using three stages in the wavelet decomposition (with five stages the limit is slightly above 18). A particularly remarkable result is the optimum 6/6 filter, because, despite its small number of coefficients (the kernel is $[2.2500, -33.4074]$), the resulting wavelet can reduce both blocking and ringing with a reasonably high performance ($G_c \times PPR = 16.67$ using three stages). Another remarkable filter is the 14/14 obtained from filter F coefficient optimization (the kernel is $[-0.4444, -3.2091, -3.1858, -7.4466, -7.2805, 116.7045]$). The results can be compared against filters from the literature, shown in the upper part of Table 2. In the examples we show results for three wavelet stages; however, the design was also tested with five and six stages, yielding consistent results. Table 3 shows the results for odd filters as well. However, as anticipated in Section 3.2, the results are not very good. The second filter of Table 3 has two zeros imposed, however, the value of the coding gain (which is related to the regularity) was not improved. Additional results using this technique can also be found in [9]–[11].

The filter coefficients were optimized using a technique that is based on the assumption that a good filter with impulse response of length L can be used to find another with length equal to $L \pm 2$. For filters small enough so that their coefficient space can be visualized, this assumption was verified to be true, (see Section 3.1). For filters with larger impulse responses, a direct verification of how close the solutions found by our procedure are to the global maximum is impractical. As an alternative to direct verification, a *simulated annealing* optimization algorithm was used, in the same fashion of the previous section, but using the objective function $F = G_c \times PPR$. The results obtained (see Table 3) present values of $G_c \times PPR$ that are very close to those obtained by our method. The largest difference in $G_c \times PPR$ values represents less than 0.4% improvement over the results of our algorithm.

Some of the wavelets designed were used to code the Lena 512×512 image using the EZW algorithm [12] at 0.15 bits per pixel. The values of *PSNR* obtained are displayed in Table 2. Wavelets iterated from optimized filters show very good values of $G_c \times PPR$, despite the lower values in *PSNR*. Note that designs based on perceptual quality may decrease the values of objective indexes, as was the case of *PSNR* (compare in Table 2 filter F before and after coefficient optimization). Also, note that the images in Figure 4 are just used to illustrate the effect of ringing and blocking reduction. The proper justification of the suitability of the objective function $F = G_c \times PPR$ was done in [13], [14].

In the first row of Figure 4, it can be seen that wavelets designed by our method (Figure 4b) show fewer blocking effects than the filter A reported in [14] (Figure 4a). This can be seen when one compares the sizes of the square

Figure 4. Lena image: (a) detail of face (128 × 128 pixel), coded at 0.15bpp using wavelets from filters A from [14] and (b) from the optimum filter of length 6/6; (c) Lena image coded with the 9/7 filter from [2] and (d) with filter F from [14] optimized for $G_c \times PPR$.

blocks on Lena's eyebrow and at the hat brim. Also, Lena's iris seem to be square in Figure 4a, and the eyelash details are poorly preserved. This improvement is primarily due to the influence of G_c in the optimization. The filter A was designed by spectral factorization of an interpolating polynomial. This example shows how the proposed process can bring improvements to short filters.

In the second row of Figure 4, it can be seen that wavelets designed by our method (Figure 4d) show less ringing than those reported in the literature (Figure 4c). The artifacts are more pronounced around the hat and around the edge of the mirror frame. This improvement can be primarily attributed to the role of the PPR in the optimization. This example shows how the proposed design process can bring improvements to long filters.

5. Conclusions

In this paper we have presented a new linear-phase biorthogonal wavelet transform design technique based on perceptual criteria. We began by presenting a method to calculate the two-band filter bank filters from just one filter, making it easier to optimize the filter bank response from the coefficients on just one filter.

The computer experiments reported in this paper lead to a better understanding of the nature of the function $F = G_c \times PPR$. Consequently, the region in the coefficient space where the best filters are located was studied, and the development of an efficient design procedure, which overcame the difficulties arising from the manifold nature of this objective function, was possible. This procedure allows a simple gradient search method to be employed. The optimization using the function $F = G_c \times PPR$ produces a perceptually improved balance between the ringing and the blocking artifacts. Conditions for performing the design using a maximum PPR condition were obtained, but the results show that maximum PPR wavelets have an inferior performance when compared to the ones optimized using $F = G_c \times PPR$.

The results presented show numerically and pictorially the improvements obtained by the optimization process.

Appendix: Procedure to calculate $H_1(z)$ from $H_0(z)$

Given an $H_0(z)$ that accepts a complementary polynomial, it is possible to calculate a unique $H_1(z)$ if its degree is less than or equal to the degree of $H_0(z)$. This can be done using equation (1) to construct a system of equations where the number of equations and the number of unknowns are the same. Each equation will force a coefficient of odd exponent from $P(z) = H_0(z)H_1(-z)$ to be zero, except for the central coefficient (z^{-2m+1}), whose coefficient is one. Even exponent coefficients are canceled in the subtraction of equation (1), i.e., $P(z) - P(-z) = 2z^{-2m+1}$.

Given the degree of $H_0(z)$, ($\deg\{H_0(z)\} = L_0 - 1$), and the degree of $H_1(z)$, ($\deg\{H_1(z)\} = L_1 - 1$), we have:

- $\deg\{P(z)\} = L_0 + L_1 - 2$ and the impulse response of $P(z)$ has length $(L_0 + L_1 - 1)$;
- The exponent of the center coefficient of $P(z)$ is $(L_0 + L_1 - 2)/2$;
- The number of equations (distinct odd terms of $P(z)$) is $(L_0 + L_1)/4$;
- The number of unknowns (distinct coefficients of $H_1(z)$) is $L_1/2$ if L_0 and L_1 are even, and $(L_1 + 1)/2$ if L_0 and L_1 are odd.

To express equation(1) in matrix form, the following practical procedure is suggested. First, construct the auxiliary matrix **D** as in the following example

($L_0 = L_1 = 12$):

$$\mathbf{D} = \begin{bmatrix} h_{01} & h_{00} & 0 & 0 & 0 & 0 & 0 & 0 & 0 & 0 & 0 & 0 \\ h_{03} & h_{02} & h_{01} & h_{00} & 0 & 0 & 0 & 0 & 0 & 0 & 0 & 0 \\ h_{05} & h_{04} & h_{03} & h_{02} & h_{01} & h_{00} & 0 & 0 & 0 & 0 & 0 & 0 \\ h_{04} & h_{05} & h_{05} & h_{04} & h_{03} & h_{02} & h_{01} & h_{00} & 0 & 0 & 0 & 0 \\ h_{02} & h_{03} & h_{04} & h_{05} & h_{05} & h_{04} & h_{03} & h_{02} & h_{01} & h_{00} & 0 & 0 \\ h_{00} & h_{01} & h_{02} & h_{03} & h_{04} & h_{05} & h_{05} & h_{04} & h_{03} & h_{02} & h_{01} & h_{00} \end{bmatrix},$$

where $h_{0k} \equiv h_0(k)$. Note that $H_0(z)$ is symmetrical. We can build now a matrix $\mathbf{C}$ such that its elements are calculated as

$$c_{i,j} = (-1)^j \left(d_{i,j} + d_{i,L_1-1-j}\right),$$

where $d_{i,j}$ represents element (i, j) of matrix $\mathbf{D}$, $i \in \left[0, \frac{(L_0+L_1)}{4} - 1\right]$. If L_1 is even, $j \in \left[0, \frac{L_1}{2} - 1\right]$, and if L_1 is odd, $j \in \left[0, \frac{L_1-3}{2}\right]$. With the matrix $\mathbf{C}$ constructed as above, it can be verified that equation (13) below is equivalent to equation (1), i.e., the solution can be found by solving the linear system

$$\mathbf{Cy} = \mathbf{z}. \tag{13}$$

In equation (13), $\mathbf{y}$ represents the solution (its elements are the second half of the impulse response of the filter $h_1(n)$) and $\mathbf{z} = [0, \ldots, 1]'$.

As an example, we have for $L_0 = 12$ and $L_1 = 12$:

$$\mathbf{C} = \begin{bmatrix} h_{01} & -h_{00} & 0 & 0 & 0 & 0 \\ h_{03} & -h_{02} & h_{01} & -h_{00} & 0 & 0 \\ h_{05} & -h_{04} & h_{03} & -h_{02} & h_{01} & -h_{00} \\ h_{04} & -h_{05} & h_{05} & -h_{04} & (h_{00}+h_{03}) & -(h_{01}+h_{02}) \\ h_{02} & -h_{03} & (h_{00}+h_{04}) & -(h_{01}+h_{05}) & (h_{02}+h_{05}) & -(h_{03}+h_{04}) \\ 2h_{00} & -2h_{01} & 2h_{02} & -2h_{03} & 2h_{04} & -2h_{05} \end{bmatrix},$$

$\mathbf{y} = \begin{bmatrix} h_{15} & h_{14} & h_{13} & h_{12} & h_{11} & h_{10} \end{bmatrix}'$ and $\mathbf{z} = [0, 0, 0, 0, 0, 1]'$.

References

[1] V. Bhaskaran and K. Konstantinides, *Images and Video Compression Standards—Algorithms and Architetures*, 1st ed. Kluwer Academic Publishers, Boston, MA, 1995.

[2] A. Cohen, I. Daubechies, and J. C. Feauveau. Biorthogonal bases of compactly supported wavelets, *Comm. Pure Appl. Math.*, XLV, 485–560, 1992.

[3] C. Herley and M. Vetterli, Wavelets and filter banks: Theory and design, *IEEE Trans. Signal Process.*, 40(9), 2207–2232, Sept. 1992.

[4] N. S. Jayant and P. Noll, *Digital Coding of Waveforms—Principles and Applications to Speech and Video*, Signal Processing Series, 1st ed. Prentice-Hall, Englewood Cliffs, NJ, 1984.

[5] J. Katto and Y. Yasuda, Performance evaluation of subband coding, *Proc. 1991 Picture Coding Symposium-PCS 91*, pp. 399–403, Tokyo, Japan, September 1991.

[6] J. Katto and Y. Yasuda, Performance evaluation of subband coding and optimization of its filter coefficients, in *Visual Communications and Image Processing '91*, pp. 95–106, SPIE, 1991.

[7] T. Nguyen and P. P. Vaidyanathan, Two-channel perfect reconstruction FIR QMF structures which yield linear-phase analysis and synthesis filters, *IEEE Trans. Acoust., Speech Signal Process.*, 37(5), 676–690, May 1989.
[8] O. Rioul, Regular wavelets: A discrete-time approach, *IEEE Trans. Signal Process.*, 41(12), 3572–3579, Dec. 1993.
[9] M. A. M. Rodrigues, E. A. B. da Silva, and P. S. R. Diniz, Design of wavelets for image compression satisfying perceptual criteria, *IEE Electron. Lett.*, 33(1), 40–41, Jan. 1997.
[10] M. A. M. Rodrigues, E. A. B. da Silva, and P. S. R. Diniz, A family of wavelets for image compression satisfying perceptual criteria, *Proceedings of the IEEE International Symposium on Circuits and Systems*, vol. 2, pp. 1109–1112, Hong Kong, June 1997.
[11] M. A. M. Rodrigues, E. A. B. da Silva, and P. S. R. Diniz, Wavelet optimization for image compression using perceptual criteria, *Annals of the Fifteenth Brazilian Telecommunications Symposium-XV SBT*, pp. 390–393, Recife, PE, Brazil, September 1997.
[12] J. M. Shapiro, Embedded image coding using zerotrees of wavelet coefficients, *IEEE Trans. Acoust., Speech Signal Process.*, 41(12), 3445–3462, December 1993.
[13] E. A. B. da Silva, Wavelet transforms for Image Coding, Ph.D. thesis, University of Essex, Great Britain, June 1995.
[14] E. A. B. da Silva and M. Ghanbari, On the performance of linear phase wavelet transforms in low bit-rate image coding, *IEEE Trans. Image Process.*, 5(5), 689–704, May 1996.
[15] P. P. Vaidyanathan, *Multirate Systems and Filter Banks*, 1st ed. Prentice-Hall, Englewood Cliffs, NJ, 1993.
[16] M. Vetterli and J. Kovačević, *Wavelets and Subband Coding*, 1st ed. Prentice-Hall, Englewood Cliffs, NJ, 1995.
[17] J. D. Villasenor, B. Belzer, and J. Liao, Wavelet filter evaluation for image compression, *IEEE Trans. Image Process.*, 4(8), 1053–1060, August 1995.
[18] D. G. Luenberger, *Linear and Nonlinear Programming*, 2nd ed. Addision Wesley Publishing Company, Reading, MA, 1984.